IEEE Access
Multidisciplinary | Rapid Review | Open Access Journal

Received 22 February 2023, accepted 26 March 2023, date of publication 3 April 2023, date of current version 2 May 2023.

Digital Object Identifier 10.1109/ACCESS.2023.3263863

RESEARCH ARTICLE

Holding Force Characteristics of Preformed Helical Fitting Based on Finite Element Method

LV ZHONGBIN[1], TAO YAGUANG[2], LIU XIAOHUI[3,4], YE ZHONGFEI[2], LI HONGPAN[4], SUN YUNTAO[5], AND YAN BO[1]

[1]College of Aerospace Engineering, Chongqing University, Chongqing 400044, China
[2]State Grid Henan Electric Power Research Institute, Zhengzhou 450052, China
[3]Inner Mongolia Enterprise Key Laboratory of High Voltage and Insulation Technology, Hohhot 010000, China
[4]School of Civil Engineering, Chongqing Jiaotong University, Chongqing 400074, China
[5]Nanjing Electric Power Fittings Design and Research Institute Company Ltd., Nanjing 210009, China

Corresponding author: Liu Xiaohui (cqdxlxh@126.com)

This work was supported in part by the Research Project of the State Grid Corporation of China under Grant 52170220001H.

ABSTRACT As an important part of transmission lines, preformed helical fitting plays an indispensable role in the safe and stable operation of electronic circuits. However, due to the poor service environment of transmission lines, preformed helical fitting can often slip, scatter, and detwist. This paper explores variations in the holding force of the preformed helical fitting under different geometric parameters. First, the geometric structure of preformed helical fitting is analyzed, and the secondary development is conducted using the ABAQUS finite element software. The script program is written in Python language to realize the parametric modeling. Based on the experimental results, the changing trend of the holding force is consistent, which confirms the correctness of the finite element model. In addition, the preformed helical fitting is studied under different values of molding aperture, pitch length, pitch number, and armor rod diameter, and changes in the holding force under different parameters are analyzed. The results show that the holding force of the preformed helical fitting increases with the decrease in the molding aperture and pitch length, and the molding aperture has a negative linear correlation with the overall holding force. The holding force increases linearly with the pitch number; so, reducing the pitch length can increase the holding force of preformed helical fitting. Moreover, the results indicate that the holding force increases with the armor rod diameter. The research results presented in this study have important guiding value for the design of performed helical fitting.

INDEX TERMS Preformed helical fitting, armor rod, pitch length, finite element method, holding force.

I. INTRODUCTION

With the advancement of China's ''West-to-East Power Transmission Project'' and ''North-to-South Power Transmission Project'' and the implementation of the development strategy of ''Three Types, Two Networks, and World Class,'' the total mileage of transmission lines of 110 kV and above in China has reached more than 655,000 km. Of them, ultra-high-voltage (UHV) transmission lines of more than 500 kV have reached more than 60,000 km, which poses higher requirements and challenges to high-voltage overhead transmission lines.

The associate editor coordinating the review of this manuscript and approving it for publication was S. Ali Arefifar.

As a core of the power system, transmission lines play an immeasurable role. With the wide application of the preformed helical fitting, due to the conductor ice, wind, and other factors, preformed helical fitting could be damaged by unbalanced tension, which could eventually lead to the outage of transmission lines. According to available statistics data, a total of 57 ground wire faults were found through the investigation of ground wire fitting accidents in the existing UHVDC (Ultra High Voltage Direct Current) projects, such as Xiangshang line, Jinsu line, Xizhe line, Hazheng line, Lingshao line, and Jiuhu line. Of 57 ground wire faults, 37 were preformed helical fitting faults, as shown in Fig. 1. The rest were other types of faults, such as ground wire bracket deformation, ground wire strand, and anti-vibration

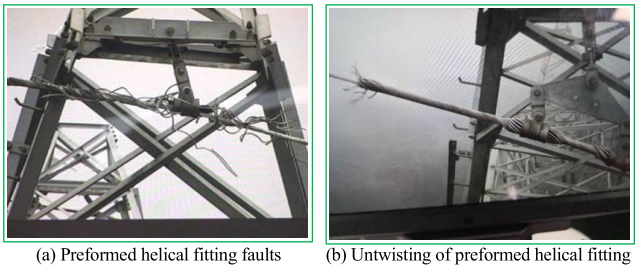

(a) Preformed helical fitting faults (b) Untwisting of preformed helical fitting

FIGURE 1. Preformed helical fitting accidents of the built UHVDC project.

hammer faults. Ground wire clamp and tension string faults occurred five times, while suspension string faults occurred 32 times.

Therefore, it is necessary to improve the preformed helical fitting performance, but there have been fewer studies on the holding force of the preformed helical fitting, and the related theory has also been lacking [1], [2]. The preformed helical fitting structure is similar to steel strand and overhead conductors for transmission lines; so, the related research on steel strand and overhead conductors for transmission lines has important reference value [3], [4].

Helical structures are widely applied in engineering and biological. Phillips et al. [5] determined the stress of each steel wire in a wire rope when the core of the wire rope is an independent steel wire. Based on this, a wire rope with six strands of 25 steel wires per strand was simulated. Jiang et al. [6], [7], [8] established a simple three-layer vertical spiral wire rope finite element model. By applying axial load (tension and torsion), the relationships between load and strain and between load and torsion of the wire rope were analyzed. Stanova et al. [9], [10] considered the single- and double-helix structures in the strand and proposed the geometric mathematical models of single- and double-layer wire ropes with initial parameters and then deduced an equation with variable parameters to determine the center line of an arbitrary circular wire. Han et al. [11] proposed a theoretical model which can calculate the global and local mechanical properties of the multilevel helical structure. Zhang et al. [12] created two finite element models to study the effect of friction on the bending stiffness of a cable consisting of a straight core wound around by a layer of helical wires. The results show that the initial bending stiffness is sensitive to the imperfect contact between the components. Based on the derivation of the local deformation parameters of a single wire, Xiang et al [13] developed an analytical model characterizing the elastoplastic behavior of wire rope and multi-strand wire rope. Moradi et al. [14] studied failures of multiple wire ropes for rig hooks and conducted a detailed failure investigation through metallographic examination and calculation analysis using the finite element method. Wu et al. [15] established a finite element model of spiral rope under tensile load using the established parameter equation. Three-dimensional geometric models of different twisting methods and equal diameter steel wires were created and analyzed using Pro/Engineer software. Meng et al. [16] used an innovative semi-analytical method to establish the wire rope model. Cen et al. [17] simplified a three-layer (1 + 6 + 12) monofilament into a one-layer monofilament via numerical simulation. Hristo et al. [18] studied the bending behavior of wire rope hangers on small-diameter rigid bodies. It can be seen from the above research results that due to the complex local contact of interwire and global mechanical behaviors of helical structures, it is difficult to study it by theoretical methods [19]. The numerical method can be used to analyze complex contact problems. However, because contact is a nonlinear problem, it will cause convergence difficulties. Therefore, the mechanical model needs to be reasonably simplified [20], [21].

In recent years, with the increase of line faults, the numerical simulation method has been used to study the stress characteristics, fatigue and wear of aluminum stranded wire [22], [23]. Liu et al. [24] proposed a finite element modeling method of the ground wire-clamp system including armor rod and aluminum armor tape. The results shows that the method can obtain accurate calculation results. Zhang et al. [25] established a finite element model of structure field for the steel core of conductor by full-tension splice to calculate the relationship between temperature and equivalent plastic strain. Guo et al. [26] established a finite element model of ACSR to obtain the temperature distribution. Rocha et al. [27] combined theory and experimental methods to study contributions on fatigue of contacting wires of overhead conductors. A finite element-based contact model combined with a nonlocal Smith-Watson-Topper criterion developed by Matos et al. [28] was used to estimate fatigue life of 6201 aluminum alloy wire of overhead conductors. Based finite element model, Belkhabbaz et al. [29] presented an approach to simulate the mechanical behavior at contact points in high-voltage electrical conductors. Lalonde et al. [30] presented an efficient finite-element modeling approach providing a full 3-D representation of both the conductor and suspension clamp and proved the validation of the finite-element modeling approach based on experimental data. Frigerio et al. [31]. presented a 3D finite element modelling to investigate the axial force-elongation behavior of a stranded conductor used for high voltage overhead lines. The validation of the 3-D finite element model is verified by comparison to corresponding measurements. Omrani et al. [2] proposed an innovative method for assessing the fatigue life combining a numerical approach based on modeling the clamp/conductor assembly using the finite element method and an experimental one. Although the above research results are mainly aimed at steel core aluminum strand, the research method can be used for the analysis of preformed helical fitting.

Luo et al. [32] believed that preformed helical fitting was an innovation in the field of a circuit in terms of force and simple construction operation. The test results showed that there was a large uniform grip between the supporting preformed armor rods and the wire, which addressed the shortcomings of the traditional metal stress concentration,

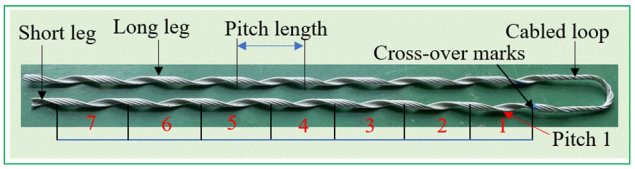

FIGURE 2. Preformed helical fitting.

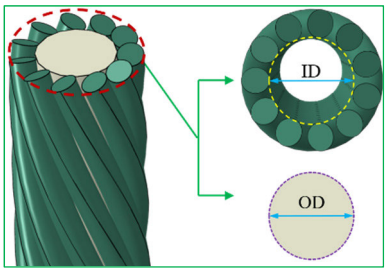

FIGURE 3. ID and OD size diagram.

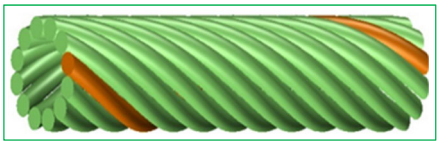

FIGURE 4. A pitch diagram of preformed armor rods.

and it was not easy to slip along the wire. Further, Li et al. [33] believed that the factors affecting the preformed helical fitting performance included the ID/OD size, pitch, sanding, helical direction (the twist direction of the outermost layer of a guiding line or optical cable; clockwise direction for the right rotation and vice versa), length, and raw materials. preformed helical fitting could greatly improve work efficiency and reduce construction costs, thus having a great effect on traditional fittings and bringing innovative vitality to China's power construction.

To solve the problem of frequent failure of preformed helical fittings caused by increased transmission line mileage and extreme weather. This paper is based on the ' ± 800 kV Lingshao DC Pole II Line 3060 Tower' event, which was caused by the slip fault of the small side preformed helical fitting. The main contributions of this work are as follows:

(1) Using the Cartesian coordinate system and the spatial geometric transformation of preformed helical fitting, the parametric equations of the preformed helical fitting and wire centerline are established. The parameter equation code of the preformed helical fitting and wire centerline is written in Python, and the finite element simulation model is obtained by importing the ABAQUS running code.

(2) Then, the finite element model is set with the test parameters consistent with the type of operating modes, and the finite element simulation and experimental results are compared to verify model accuracy.

(3) Finally, the control variable method is used to calculate and analyze the influence of the four parameters, i.e., molding aperture, length, pitch, and diameter, on the fastening performance of preformed helical fittings. The results provide reference for research into the design of the preformed helical fitting.

II. GEOMETRIC MODEL OF PREFORMED HELICAL FITTING

The preformed helical fitting is widely used in power transmission lines. Its main function is to tighten the conductor and install it on the terminal tower. The preformed helical fittings can avoid damage to the conductor due to stress concentration and improve the life of the conductor. This preformed helical fitting is simple in structure and easy to install. The premise of its normal and stable operation is to ensure sufficient holding force, as shown in Figure 2.

The first process of the preformed helical fitting processing design is structure molding, which is to use a specific mold to twist multiple preformed armor rods of a specific size in the same spiral direction to form a coaxial strand structure and then cut them into a preformed armor rod at a certain length and a specified molding aperture. After a series of processes, including grouping, cleaning, mucilage glue, sandblasting, stranding, and bending. The cavity inner diameter *ID* of preformed helical fitting is smaller than the matching wire outer diameter *OD*, as shown in Figure 3. In this way, uniform compressive stress is generated in the contact area between the two, and then, it is transformed into mutually constrained friction force so that the preformed armor rod harness is tightly wound on the wire or cable; thus, the fastening performance of the preformed helical fitting is formed [34].

The two factors affecting the fastening performance of the preformed helical fitting are the environmental conditions of service and the structural parameter factors of the preformed helical fitting, which include the pore size, length, pitch, and diameter of preformed armor rod molding, where the pitch is the axial length of a preformed armor rod molding a complete spiral in the strand, as shown in Figure 4. Due to the uncontrollability of a service environment of the preformed helical fitting, this study focuses on the influence of various structural parameters on the fastening performance of the preformed helical fitting.

A. GEOMETRIC PARAMETERS OF PREFORMED HELICAL FITTING

The preformed helical fitting structure is complex. Therefore, to establish an accurate and reasonable mathematical model, it is necessary to study its cross-sectional distribution. The model establishment process is conducted using a parametric method, which avoids the repeated operation of a large amount of conventional work, effectively improves modeling efficiency, and is more conducive to studying the fastening performance of the preformed helical fitting under different parameters.

The technological process of twisting the preformed armor rod around the central transmission line into strands by

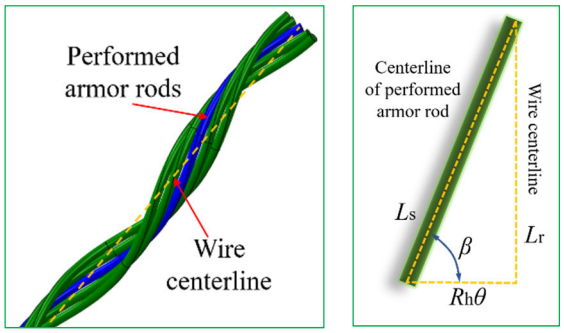

(a) Spiral preformed armor rods (b) Plane expansion diagram of a single preformed armor rod

FIGURE 5. Schematic diagram of the preformed armor rods on the spiral and expansion planes.

special mechanical equipment becomes strands. The spiral winding direction of a preformed armor rod is called the twisting direction. The length of the spiral line with a point on the side strand preformed armor rod winding the axial rotation angle of the wire of 360° is called the pitch and is denoted by S. The length of the vertical line from the point on the side strand preformed armor rod central line to the central transmission line axis denotes the spiral radius R_h. The ratio of pitch S to wire diameter D is called pitch multiple K, and it is calculated as follows:

$$K = \frac{S}{D} \tag{1}$$

The central axis of a preformed armor rod wrapped in the same direction in the preformed helical fitting is a helix. The plane expansion diagram of preformed armor rods is shown in Figure 5. The linear length of the preformed armor rod along the axial direction is Lr. The length expanded in the spiral direction is Ls. The angle between the side preformed armor rod and the axial direction of wire is the twist angle β. The angle around the transmission line is θ. The correlation function relationship is as follows:

$$\tan\beta = \frac{L_\mathrm{r}}{R_\mathrm{h}\theta} \tag{2}$$

Due to the existence of twist angle β in preformed helical fitting, the cross-section of preformed armor rods is not circular but approximately elliptical [35], [36], as shown in Figure 6(b). The relationship between radius is $R_h = R_c + R_w$, where R_h is the total radius, R_c is the wire radius, and R_w is the outer armor rod radius.

B. GEOMETRIC MODELING OF PREFORMED HELICAL FITTING

The computer programming language Python was used to model the preformed helical fitting, and the simulation analysis was conducted using the ABAQUS finite element software. Accurate mathematical models are crucial and directly determine the reliability of all subsequent calculations.

First, the geometric transformation was performed with reference to the helical spring [37], [38]. A rectangular

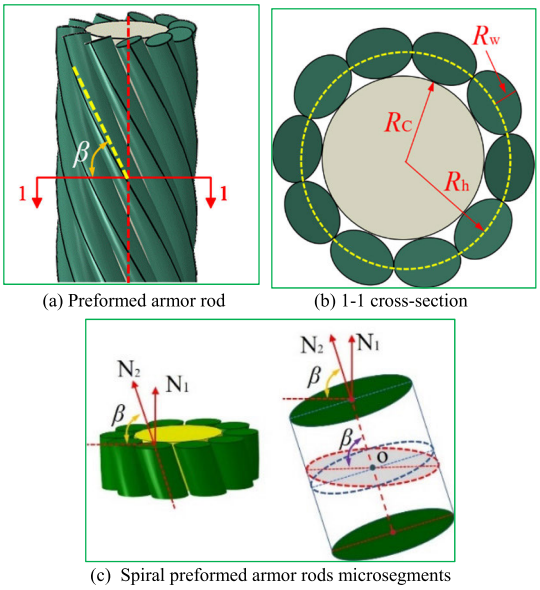

(a) Preformed armor rod (b) 1-1 cross-section

(c) Spiral preformed armor rods microsegments

FIGURE 6. Three-dimensional geometric configuration and micro-element diagram of the preformed helical fitting.

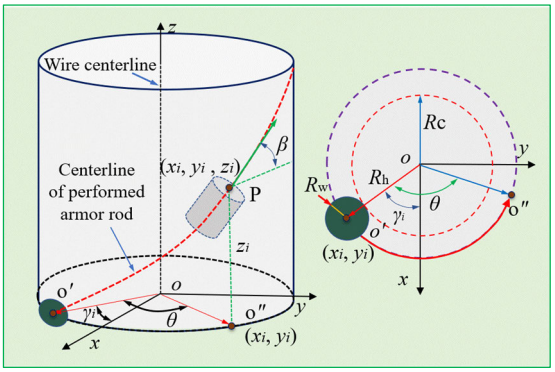

FIGURE 7. Center line of the preformed helical fitting in the right-hand direction of the winding z-axis.

Cartesian coordinate system (0; x, y, z) in three-dimensional Euclidean space defines point P uniquely by the ordered triple of numbers [x, y, z], where x, y, and z denoted the Cartesian coordinates of point P.

As shown in Fig. 7, the point o´($R_\mathrm{h}\cos(\gamma_i)$, $R_\mathrm{h}\sin(\gamma_i)$, 0) is intersection point of centerline of performed armor rod and x-o-y plane. γ_i is the included angle between o´o and x-axis. γ_i describes the position of i-th performed armor rod. P is a point on the centerline of performed armor rod. o'' is a point projected onto the x-o-y plane by P in space. θ is the included angle between o´o and o''o. θ is the angular displacement generated by movement of the point on centerline of the performed armor rod.

Equation 3 defines the geometric model of preformed helical fitting with any geometric size:

$$\begin{aligned} x_i &= R_\mathrm{h}\cos(\gamma_i + q\theta) \\ y_i &= R_\mathrm{h}\sin(\gamma_i + q\theta) \\ z_i &= \frac{R_\mathrm{h}\theta}{\tan(\beta)} \end{aligned} \tag{3}$$

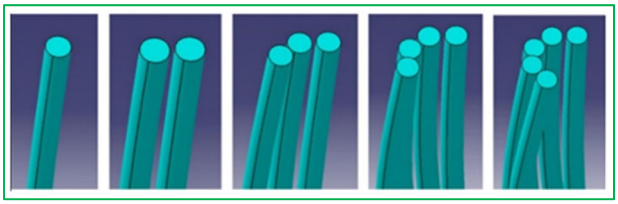

FIGURE 8. Preformed armor rods with different root numbers in a layer.

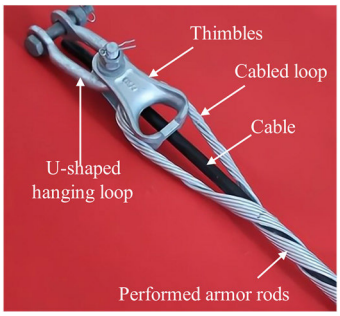

FIGURE 9. Preformed helical fitting.

In formula (3), (x_i, y_i, z_i) is the spatial coordinates of any point on the central axis of the i-th preformed armor rod. When $q = 1$, it means that the preformed armor rod is wound in a right-handed manner. If $q =$ -1, it means that the preformed armor rod is wound in a left-handed manner.

By setting the size, material properties, and contact types of preformed helical fitting, a layer of preformed armor rods with different root numbers was finally assembled in the finite element software ABAQUS, as shown in Figure 8.

III. FINITE ELEMENT MODELING OF PREFORMED HELICAL FITTING BASED ON ABAQUS

A. FINITE ELEMENT MODEL OF PREFOMED HELICAL FITTING

1) GEOMETRIC MODELING AND MATERIAL PROPERTY

The preformed helical fitting was used to fix the wire, withstand the wire tension, and hang the wire to the tension string or tower. The installation setup is shown in Figure 9, where it can be seen that it consisted of preformed armor rods, a heart-shaped tension ring, and a U-shaped hanging ring. Before fixing the wire, the preformed armor rod bundle was twisted into an empty pipe, and then, the wire was placed in the preformed armor rod bundle. The wire clamp was connected with the insulator string through the heart-shaped tension ring; so, the preformed armor rod bundle could produce a strong grip to fix the wire. In the finite element software ABAQUS, the wire model was simplified under the premise of fully reflecting the mechanical properties of the preformed helical fitting. According to the actual position, the transmission wire and preformed armor rod bundle components were assembled. The simplified model is shown in Figure 10.

In practice, a transmission line represents a component composed of multiple non-insulated single wires for current transmission, with a concave and convex surface. However, this study does not consider the influence of the surface effect of the transmission lines on the fastening characteristics.

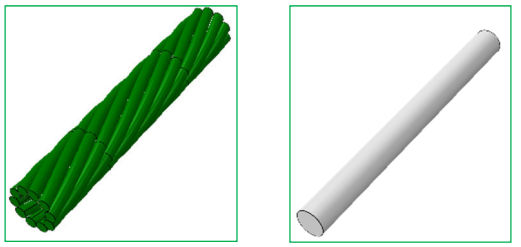

(a) Preformed helical fitting model diagram (b) Cable model diagram

FIGURE 10. Finite element model of the preformed helical fitting.

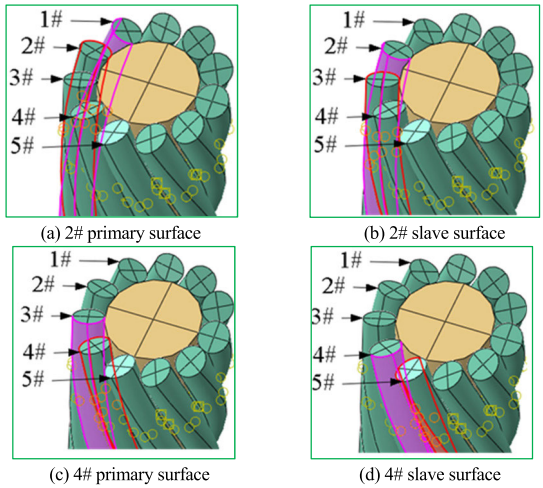

(a) 2# primary surface (b) 2# slave surface

(c) 4# primary surface (d) 4# slave surface

FIGURE 11. Schematic diagram of binding constraints of adjacent preformed armor rods.

2) INTERACTION RELATIONSHIP DEFINITION

To eliminate the rigid body displacement and reduce the number of iterations required to calculate the contact state, the preformed armor rod bundle was defined as a whole common force without relative motion. Therefore, the adjacent preformed armor rods were bound in turn, as shown in Figures 11 and 12.

The preformed armor rod 4# shown in Figure 11(d) defined the surface adjacent to the preformed armor rod 3# as the primary surface, and the surface adjacent to the preformed armor rod 5# was set as a slave surface. In addition, the position tolerance was set to be slightly larger than the distance between the primary and slave surfaces to ensure effective binding.

Next, the contact attribute was defined, and the default hard contact was used in a normal behavior, that is, the contact pressure that could be transmitted between the contact surfaces was not limited. When the contact pressure became negative or zero, the two contact surfaces separated, and the contact constraints on the corresponding nodes were overcome.

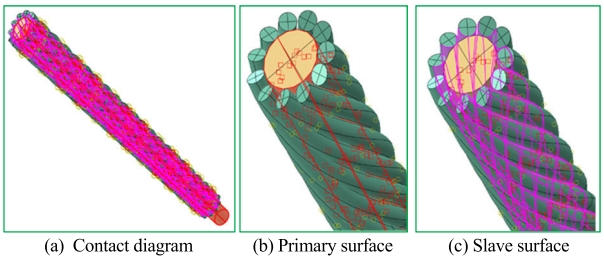

FIGURE 12. Master and slave surfaces of the contact area of the preformed helical fitting.

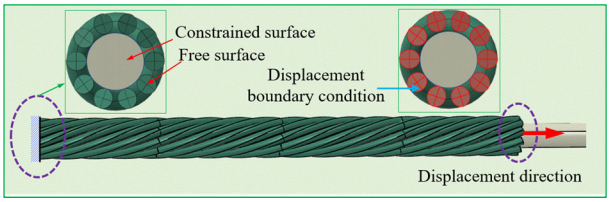

FIGURE 13. Boundary condition constraint and loading of the model.

3) BOUNDARY CONSTRAINTS AND LOAD APPLICATION

In the finite element software ABAQUS, three analysis steps were set as follows. The first step defined the contact between the conductor and the preformed armor rod; the second step simulated the preload between the wire and the preformed armor rods; the third step performed the drawing simulation of the preformed armor rod, and the maximum reaction force at the drawing displacement point of the preformed armor rod was recorded. According to the interaction relationship of the force, the maximum reaction force value corresponded to the drawing resistance of the preformed armor rod, namely the holding force.

According to the actual engineering installation of preformed helical fitting, as shown in Figure 10, the wire at the end that was parallel to the preformed armor rods near the central tension ring was fixed, and a reference point RP-1 was established at the center of the wire end face. The relationship between the reference point and the end face was established through coupling; the freedom of reference point 1 in six directions was limited, while the other end of the wire was free. The axial tensile displacement load was applied to the preformed armor rod end of the free end of a conductor [22]. A new reference point RP-2 was determined in the axis direction of the preformed armor rods, and the coupling connection between the new reference point and the preformed armor rod end face of the free end of the wire was established through coupling. This restricted the displacement and rotation of PR1, and the other end of the preformed armor rods was free. The boundary condition constraints and load setting of the model are shown in Figure 13.

4) MODEL GRID DIVISION AND SENSITIVITY ANALYSIS

Since the concave and convex characteristics of the conductor were ignored, there were many contact surfaces in the model.

TABLE 1. Finite element model parameters for mesh sensitivity analysis.

Group no.	D_w (mm)	D_c (mm)	Mesh size (S_w/S_c(mm))	Pitch length(mm)
1	5.2	15.8	1.0/2.0	
			1.1/2.2	170
2	3.6	11.4	1.2/2.4	180
			1.3/2.6	190
3	7.0	20.0	1.4/2.8	

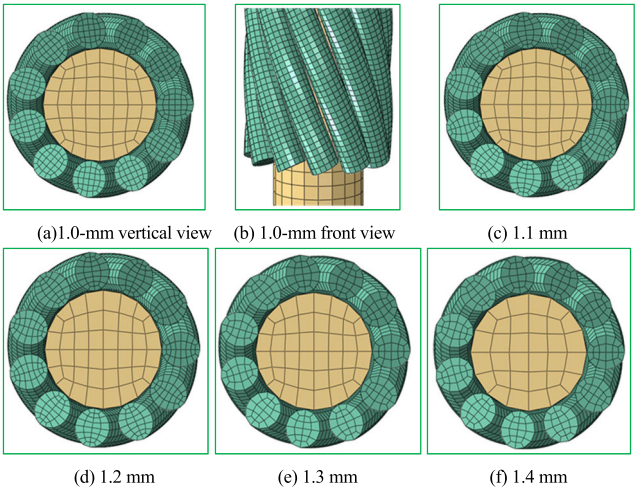

FIGURE 14. Finite element model of the preformed armor rods with different mesh sizes.

To improve the accuracy and correctness of analysis, the hexahedral linear reduction integral element C3D8R was selected for the grid.

In this section, the effect of the mesh on the fastening performance of the preformed helical fitting is studied under the condition of constant values of molding aperture, preformed armor rods length, pitch, and diameter. To increase the reliability of the simulation, three operating modes were selected. In addition, to avoid the contingency of simulation, pitch lengths of 170 mm, 180 mm, and 190 mm were selected for each case. As shown in Table 1, there were 45 operating modes. As shown in Fig 6, D_c is the wire diameter, and D_w is the diameter of the outer armor rod. In Table 1, S_c is the mesh size of the wire, and S_w is the mesh size of the outer armor rod. As shown in Figure 14, the size of the preformed armor rods was set to the following values: 1 mm, 1.1 mm, 1.2 mm, 1.3 mm, and 1.4 mm.

The simulation results for the 170-mm pitch of preformed armor rods under condition 1 were selected. The mesh sizes of preformed armor rods were 1 mm, 1.1 mm, 1.2 mm, 1.3 mm, and 1.4 mm, and the numbers of units in the corresponding model were 128,772, 105,636, 68,024, 64,020, and 57,680, respectively. The contact pressure under different grid sizes is shown in Figure 15.

As shown in Figure 15, the maximum contact pressure was 1,148 MPa, 947.5 MPa, 738.0 MPa, 730.4 MPa, and

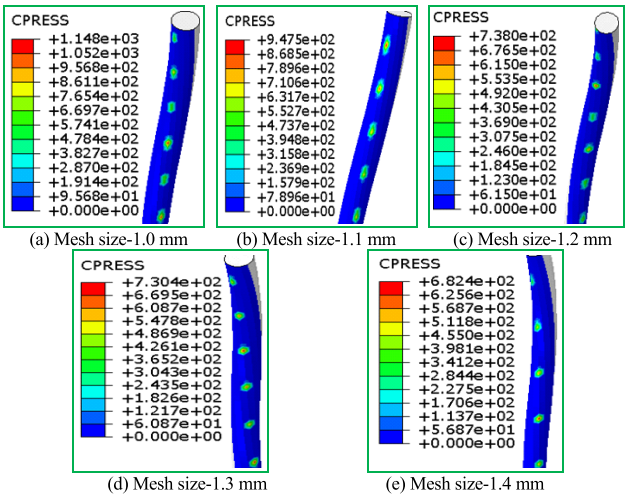

FIGURE 15. Contact pressure contours under different preformed armor rod mesh sizes.

682.4 MPa under the mesh sizes of 1.0 mm, 1.1 mm, 1.2 mm, 1.3 mm, and 1.4 mm, respectively.

Next, the sensitivity of the model grid size was analyzed. By changing the model grid size, the changing trends of the holding force and normal contact pressure (CPRESS) of the preformed helical fitting were analyzed under various operating modes. The results are shown in Figure 16.

As shown in Figure 16, the changing trends of the holding force and contact pressure with the mesh size under three operating modes were as follows. With the increase in the model mesh size, CPRESS value between the wire and the preformed armor rods increased gradually, that is, the more ideal the contact state was, the larger the holding force value was. This was because the mesh could be divided into dense parts so that the theoretical value of holding force became a stable value, which was the ideal result, but the contact of this model was complex, and the computer calculation was limited by bits. The model mesh under the above conditions was not completely refined. The finer the mesh, the more the holding force value. Other conditions were the same, and the change trend of holding force and CPRESS value with mesh size was the same under different pitches, indicating that the grid had no effect on the overall changing trend of the holding force. Therefore, in the subsequent calculation, an appropriate mesh size was selected according to the specific conditions. For instance, the mesh size of the model could be slightly increased when simulating the long preformed armor rod to ensure the accuracy of calculation results and improve the calculation efficiency.

B. VERIFICATION OF FINITE ELEMENT MODEL OF PREFORMED HELICAL FITTING

According to the Chinese technical standard "Technical requirements for overhead line helical fittings (DL/T763-2013)", the holding force of preformed helical fitting should not be less than 95% of the rated breaking force of supporting cables. The preformed helical fitting with model NL-150BG-20 (HZ-122007) was selected as the research object in the experiment. As shown in Figure 17, the LBGJ-150-20AC cable with an outer diameter of 15.8 mm was selected as the matching wire material for the aluminum-clad steel strand. The tested preformed helical fitting was installed on the tension machine flatly, as shown in Figure 18. In no less than 30 seconds, the external force was loaded to 50% of the rated tension of the wire, and it was kept for 2 minutes before loading to the specified holding force (95% of the rated tension of the wire), and then kept for 1 minute. During the experiment, there was no slippage between the inner and outer layers of the preformed armor rods, and both the wire and the preformed helical fitting were damaged, which was regarded as a successful experiment.

The main parameters affecting the holding force of preformed helical fittings were studied from four aspects, namely, molding aperture, preformed armor rod length, pitch, and diameter. Combined with the size of preformed armor rod molding die, eight groups of operating modes were set, as shown in Tables 2. As shown in Fig 3, Inner diameter *ID* is the aperture of preformed helical fitting, *OD* is the wire outer diameter. In Table 2, the fifth column is the pitch length of preformed helical fitting, the sixth column is the total length of performed helical fitting. In addition, to reduce accidental errors in the experiment, three experiments were conducted for each sample number. The experimental results are shown in Table 3.

Next, a simulation model was constructed based on the above experimental conditions according to the relevant parameter settings of the aforementioned preformed armor rods model. However, due to the limitations of the current

TABLE 2. Eight experimental conditions.

Test no.	D_w (mm)	*ID* (mm)	*ID*/*OD*	Pitch length (mm)	Total length (mm)
1#	Φ5.2	Φ13.1	0.83	180	1,600
2#	Φ5.2	Φ13.4	0.85	180	1,600
3#	Φ5.2	Φ13.7	0.87	180	1,600
4#	Φ5.2	Φ13.1	0.83	185	1,060
5#	Φ5.2	Φ13.1	0.83	185	1,240
6#	Φ5.2	Φ13.1	0.83	185	1,600
7#	Φ5.2	Φ13.1	0.83	190	1,600
8#	Φ4.8	Φ13.1	0.83	180	1,600

TABLE 3. Experimental results of the holding force of the preformed armor rods for each sample.

Test no.	1 Holding force (kN)	2 Holding force (kN)	3 Holding force (kN)	Average holding force (kN)
1#	193.8	192.1	193.2	193.0
2#	192.1	192.2	192.0	192.1
3#	194.1	186.9	193.8	191.6
4#	123.3	123.5	133.3	126.7
5#	162.4	156.8	159.1	159.4
6#	188.7	192.2	193.0	191.3
7#	185.7	186.8	187.5	186.7
8#	188.6	194.4	193.2	192.1

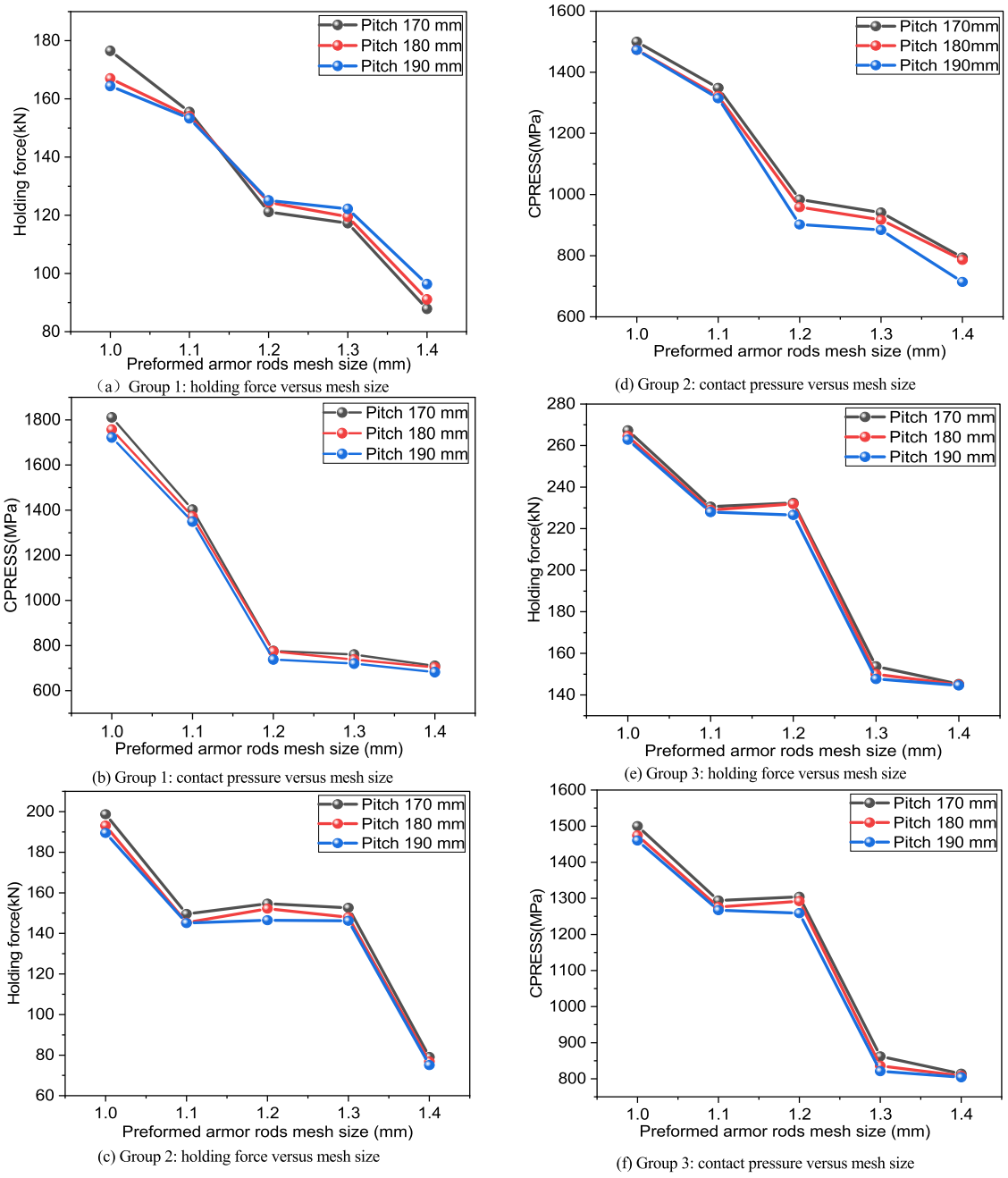

FIGURE 16. **Simulation results of different mesh sizes under different operating modes.**

simulation, it was impossible to simulate a small molding aperture in the test. In the simulation, the molding aperture diameters of 15.68 mm, 15.70 mm, and 15.72 mm were used in turn, while the other parameters were kept the same. The simulation results of the clamping force and stress of the preformed helical fitting for different diameters are shown in Figure 19.

According to the simulation results obtained by the ABAQUS software, the experimental and simulated holding force values obtained under different parameters were compared, as shown in Figure 20.

As shown in Figure 20, the changing trend of the holding force under all conditions was consistent compared with the experimental and simulation results. For instance, the changing trend of the holding force for a 13.4-mm molding aperture, 1240-mm length, and 185-mm pitch was the same. The simulation results have a reference value, indicating that the model parameter setting is reasonable. Considering the inevitable experimental errors, the calculation accuracy of the model has met the requirements. The results of this research have practical engineering reference value and can be used for subsequent simulation.

FIGURE 17. Preformed helical fitting sample used in the experiment.

FIGURE 18. Tensile testing machine used in the experiment (from the company project test diagram).

C. PARAMETER EFFECT ANALYSIS OF HOLDING FORCE OF PREFORMED HELICAL FITTING

1) MOLDING APERTURE EFFECT ON HOLDING FORCE OF PREFORMED HELICAL FITTING

According to the tightening performance principle of a preformed helical fitting, the inner diameter ID of a cavity formed by the preformed armor rods is less than the inner diameter OD of a wire. For the convenience of a uniform description, the difference between the two was introduced, i.e., the difference margin, denoted by Δ f. its value was set as follows: $\Delta f = 0.08$ mm, 0.10 mm, 0.12 mm, and 0.14 mm. The larger the difference was, the smaller the pore size was, which fully reflected the variation trend of the holding force. The pitch of the preformed armor rods was changed in the range of 150–210 mm, increasing by 10 mm each iteration; the total length of the preformed helical fitting

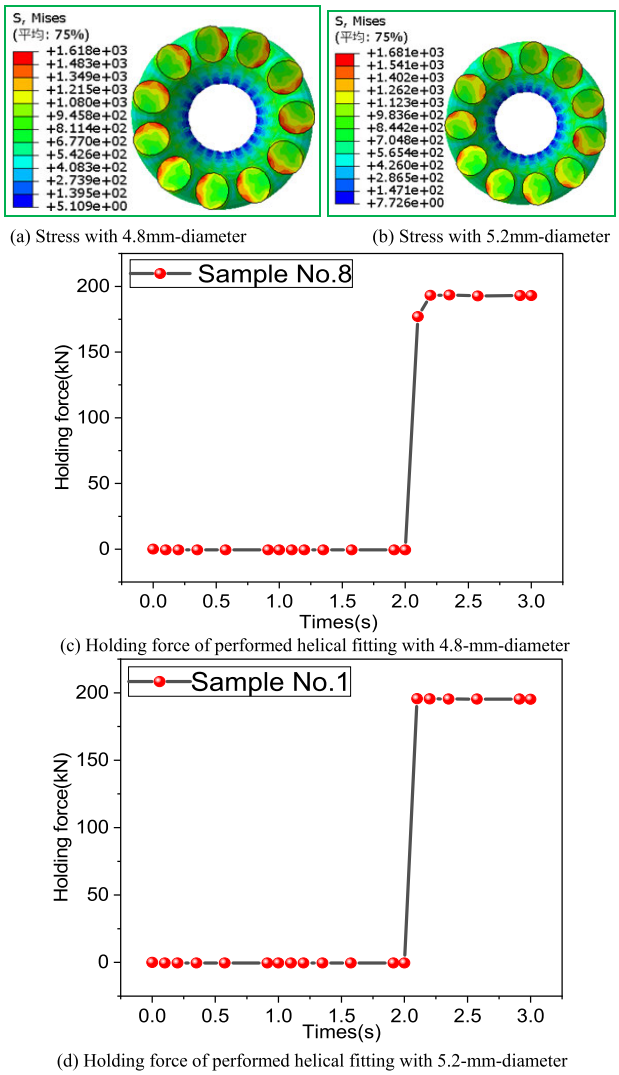

FIGURE 19. Results of the stress and holding force of the preformed helical fitting for different diameters.

TABLE 4. Finite element model parameters for molding aperture.

Group no.	D_w (mm)	D_c (mm)	*ID* (mm)	Pitch length (mm)
4	5.2	15.8	15.66, 15.68, 15.70, 15.72	150 160
5	3.6	11.4	11.26, 11.28, 11.30, 11.32	170 180
6	7.0	20.0	19.86, 19.88, 19.90, 19.92	190 200 210

was 320 mm. Under the condition of keeping the radius, pitch, raw materials, and length unchanged, a total of three groups of 84 operating modes were set to calculate and compare the changing trend of the holding force. The molding aperture value under each working condition is shown in Table 4.

Three groups of operating modes under the preformed armor rods pitch of 180 mm and difference of $\Delta f = 0.08$ mm were selected to simulate the stress nephogram, as shown

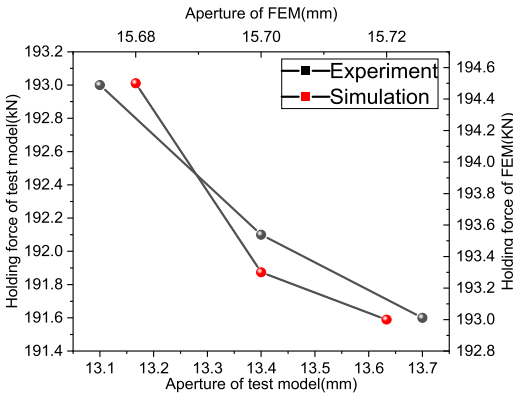

(a) Holding force versus molding aperture diagram

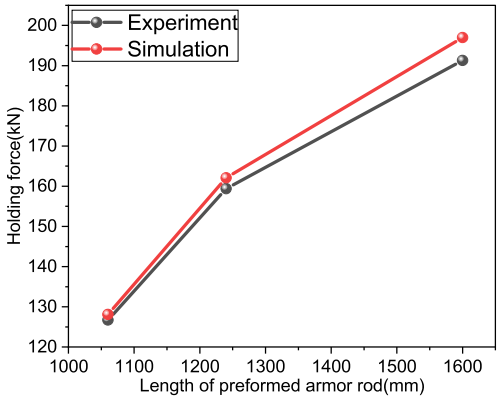

(b) Holding force versus preformed armor rod length diagram

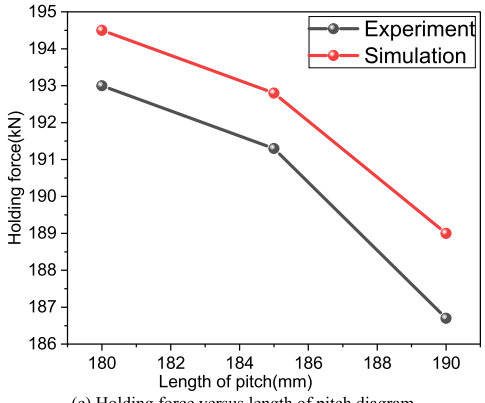

(c) Holding force versus length of pitch diagram

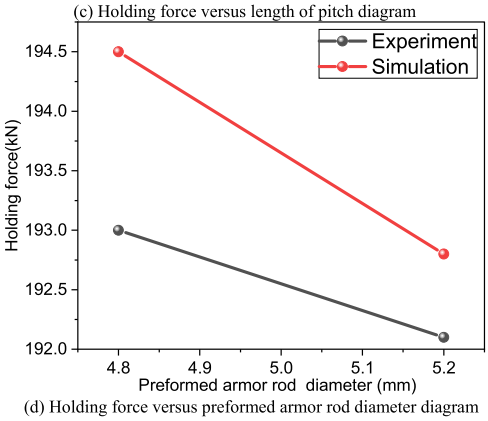

(d) Holding force versus preformed armor rod diameter diagram

FIGURE 20. Comparison of experimental and simulation results under different influence parameters.

in Table 4, and the obtained simulation results are shown in Figure 21.

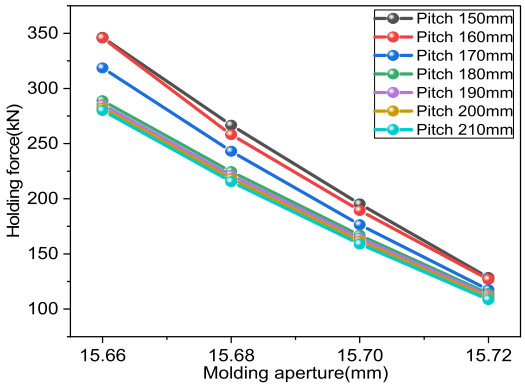

(a)Group 4: holding force versus molding aperture

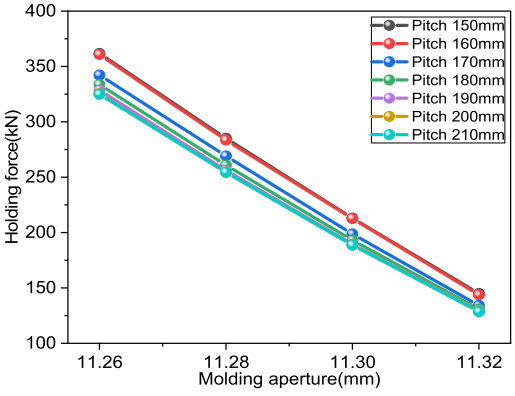

(b) Group 5: holding force versus molding aperture

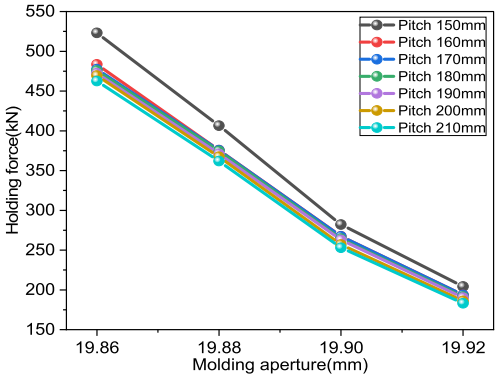

(c)Group 6: holding force versus molding aperture diagram

FIGURE 21. Relationship diagram of the holding force versus the molding aperture of the preformed helical fitting under different operating modes.

As shown in Figure 21, the larger the difference was, and the smaller the molding aperture was, the larger the holding force and stress of the preformed helical fitting were. The results indicated that the changing trend of the holding force with the molding aperture was consistent, showing a slightly negative linear relationship, which was independent of the pitch size. In the subsequent analysis, the difference of $\Delta f = 0.1$ mm was used for simulation.

2) LENGTH EFFECT ON HOLDING FORCE OF PREFORMED HELICAL FITTING

In the first case, 3-8 pitches were selected in turn, while the other parameters were kept the same. Moreover, to reflect

TABLE 5. Finite element model parameters for number of pitches.

Group no.	D_w (mm)	D_c (mm)	Mesh size (S_w/S_c(mm))	Pitch number	Pitch length (mm)
7	5.2	15.8	1.2/2.4	3,4,5	150,160
				6,7,8	170,180
8	7.0	20.0			190,200

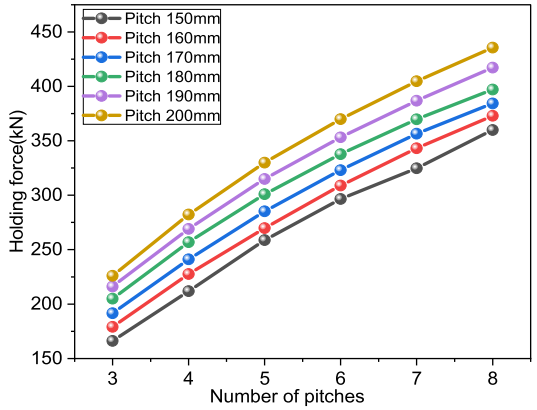

（a）Group 7: holding force versus pitch number

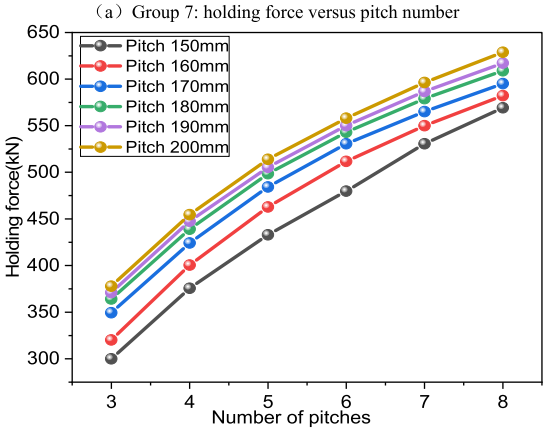

（b）Group 8: holding force versus pitch number

FIGURE 22. Relationship diagram of the holding force versus the pitch number of the preformed helical fitting under different operating modes.

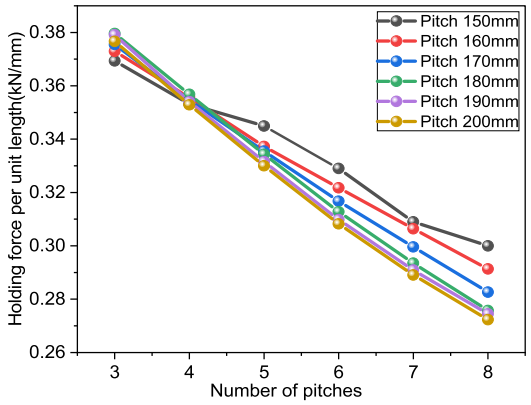

（a）Group 7: unit-length holding force versus pitch number

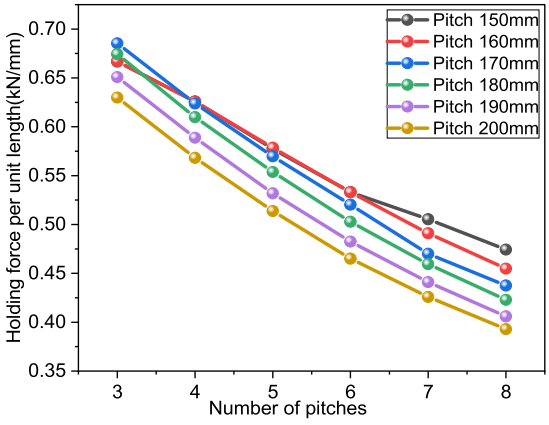

(b) Group 8: unit-length holding force versus pitch number

FIGURE 23. Relation diagram of the holding force per unit length versus the pitch number of the preformed helical fitting under different operating modes.

the changing trend of the holding force, multiple pre-twist pitch values were used, and the pitch was in the range of 150-200 mm. A total of 72 operating modes were set up and divided into two groups to analyze and compare the change in preformed helical fitting holding force. The specific operating modes are shown in Table 5.

The calculation results of the preformed helical fitting pitch of 180 mm in operating mode 7 were used to calculate the relationship between the number of pre-twisting wire pitch (length) and the holding force of the preformed helical fitting and the holding force of the unit length, as shown in Figures 22 and 23.

The results indicated that regardless of the preformed armor rod pitch value, the holding force and stress increased with the pitch number (length), and the overall trend was roughly linear. In engineering, the length of the preformed helical fitting can be appropriately increased to obtain a larger fastening performance. In addition, the holding force per unit length of the preformed helical fitting decreased with the number of pitches. In group 7, four pitches were critical, and the total number of pitches was greater than 4. The smaller the pitch value of the preformed helical fitting, the greater the holding force per unit length and the more conducive it was to saving materials, and vice versa.

In group 8, the unit-length holding force of the preformed helical fitting generally decreased with the number of pitches. Under the same conditions, the smaller the pitch value of the preformed armor rods was, the greater the unit-length holding force was. In other words, the stronger the winding was, the more difficult it was to be pulled and the more favorable it was for the project.

The relationship between the holding force and the pitch number of the preformed helical fittings under two operating modes was linearly fitted. The linear fitting was translated to the position where the pitch number was 5 and the pitch was from 150 mm to 200 mm, and the error analysis was conducted; the analysis results are shown in Figure 24.

According to the results shown in Figure 24, the fitting slopes under operating modes 7 and 8 were 39.2 and 49.8,

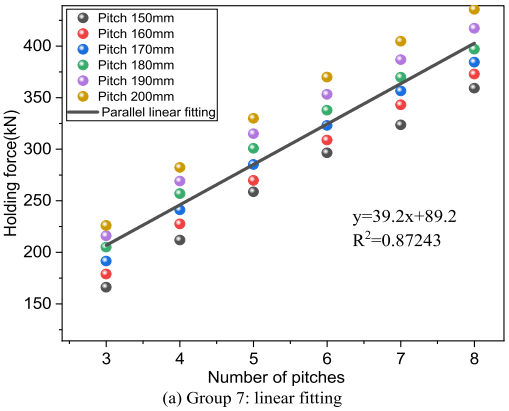

(a) Group 7: linear fitting

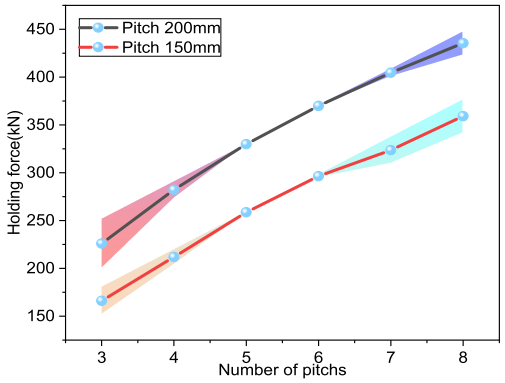

(b) Group 7: error band diagram

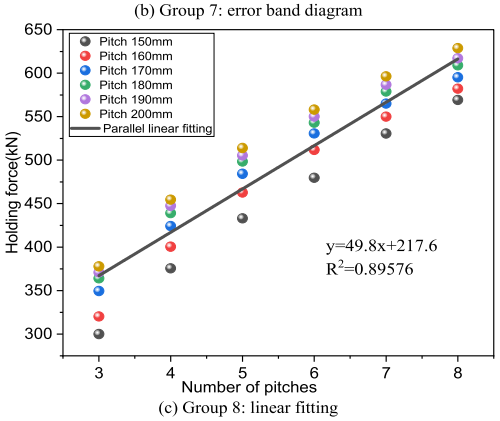

(c) Group 8: linear fitting

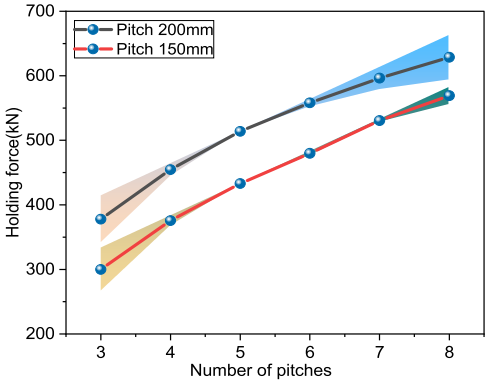

(d) Group 8: error band diagram

FIGURE 24. Linear fitting and error analysis results of the preformed helical fitting under different operating modes.

respectively. The error band diagram indicated that the error in holding force was small when the number of preformed

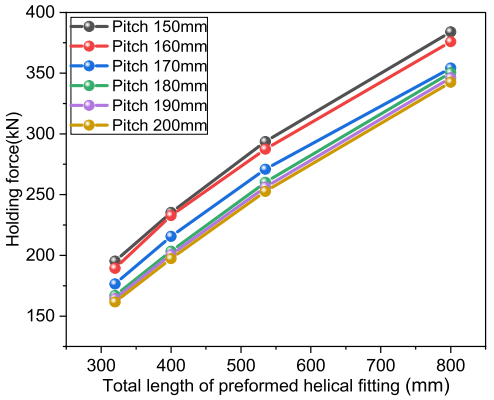

(a) Group 9: holding force versus the total length diagram

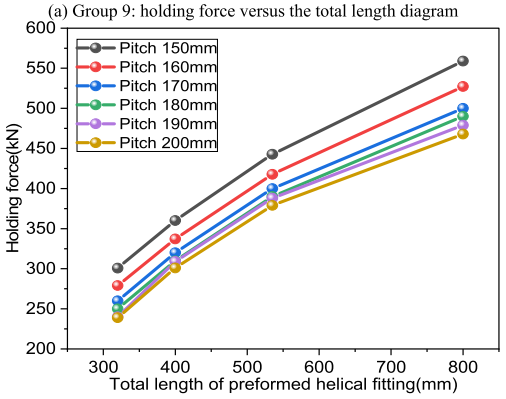

(b) Group 10: holding force versus the total length diagram

FIGURE 25. Preformed armor rod holding force versus the total rod length under different operating modes.

armor rod pitches was between 4 and 7, and the holding force could be accurately predicted. The maximum relative error of the holding force pair was calculated for three pitches. The maximum relative error in group 7 at the pitch of 150 mm and 200 mm was 8.48% and 11.33%, respectively. The maximum relative error in group 8 at the pitch of 150 mm and 200 mm was 11.13% and 9.63%, respectively. The relative error of the holding force was less than 12%, which has a certain reference value.

The second type of length changes, in addition to the above changes in the number of preformed armor rod pitch; the total length of the preformed armor rod was directly changed, while the other parameters remained unchanged. The total length of the preformed helical fitting used in the experiment was 1/5, 1/4, 1/3, and 1/2 of 1,600 mm, that is, the total length has the following values: 320 mm, 400 mm, 535 mm, and 800 mm. To reflect the changing trend of the holding force, multiple pitch values in the range of 150-200 mm were selected, and a total of 48 operating modes were set up and divided into two groups to analyze the changes in the preformed armor rod holding force. The specific operating modes are presented in Table 6. The 48 operation modes are simulated. The relationship between the holding force of the preformed helical fitting and the length of the preformed armor rod is shown in Figure 25. The relationship between the holding force per unit length and the length of the preformed armor rod is shown in Figure 26.

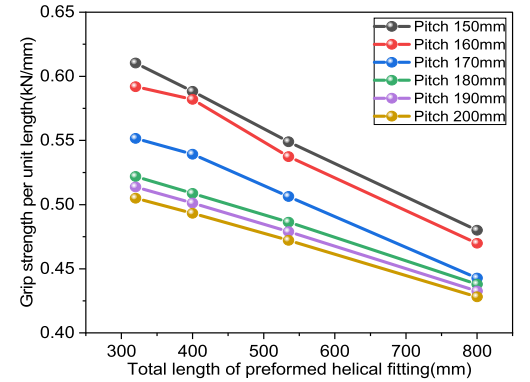

(a) Group 9: unit-length holding force versus the total length diagram

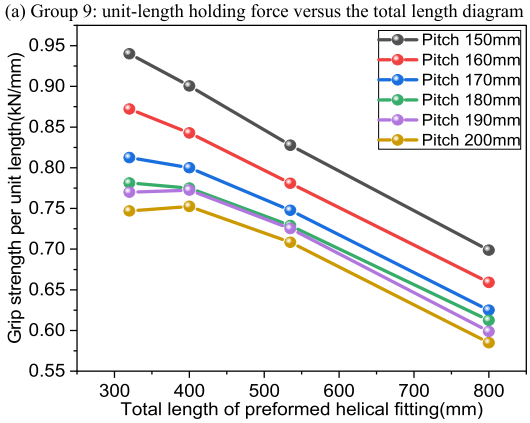

(b) Group 10: unit-length holding force versus the total length diagram

FIGURE 26. Unit holding force versus the total length of the preformed armor rods under different operating modes.

As shown in Figures 25 and 26, under the two groups of operating modes, regardless of the pitch value, the holding force and stress of the preformed helical fitting increased with the length of the preformed armor rods, and the relationship was roughly linear. In contrast, the unit-length holding force was inversely proportional to the length, and the smaller the pitch was, the better the fastening performance was. In practice, the preformed helical fitting length can be adjusted to obtain better fastening performance.

Further, the two above-mentioned methods of changing the length were used to study the fastening performance. Multiple pitch values were selected for each working condition to reflect the changing rule of the holding force fully. A total of 120 operating modes were defined and divided into four groups. The results of the four groups were consistent, which strongly confirmed the correctness of the conclusions. The analysis of the four groups' results has shown that the length has no effect on the overall changing trend of the preformed helical fitting. Therefore, under the premise of ensuring accuracy in the subsequent calculation, the appropriate preformed armor rod length simulation can be selected to improve the calculation efficiency.

3) PITCH LENGTH EFFECT ON HOLDING FORCE OF PREFORMED HELICAL FITTING

According to the previous research results, the difference was set to 0.1 mm, and the total length of the preformed helical fitting was set to 320 mm to study the effect of the pitch size on the holding force. According to the size of the experimental grinding tool, the pitch of the preformed armor rods was set to 150 mm, 160 mm, 170 mm, 180 mm, 190 mm, and 200 mm in turn. A total of 18 operating modes were defined and divided into three groups to analyze changes in the holding force of the preformed armor rods, as shown in Table 7. The results obtained under operating mode 11 are shown in Figure 27, and changes in the holding force and stress with the pitch of the preformed armor rods under the three groups of conditions are shown in Figure 28.

As shown in Figure 28, under the three operating modes, the holding force of the preformed helical fitting decreased with the pitch value. The holding force under operating mode

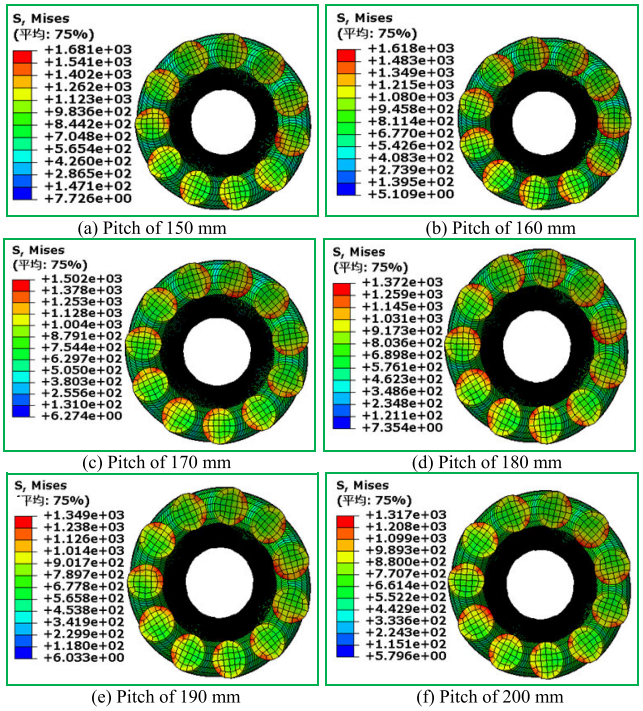

FIGURE 27. Pitch versus stress cloud under operating mode 11.

TABLE 6. Finite element model parameters of working conditions 9 and 10.

Group no.	D_w (mm)	D_c (mm)	Mesh size (S_w/S_c(mm))	Total length (mm)	Pitch length (mm)
9	2.6	7.9	1.0/2.0	320 400	150,160 170,180
10	3.5	10.0		535 800	190,200

TABLE 7. Finite element model parameters of working conditions 12-13.

Group no.	D_w (mm)	D_c (mm)	Mesh size (S_w/S_c(mm))	Pitch length (mm)
11	5.2	15.8	1.0/2.0	150,160
12	3.6	11.4		170,180
13	7.0	20.0		190,200

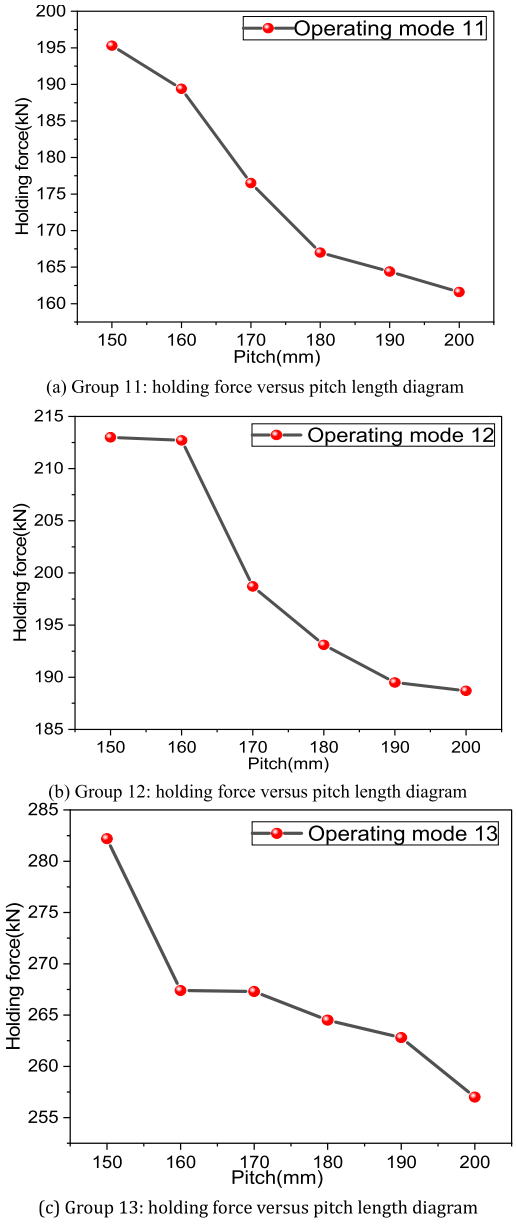

FIGURE 28. Results of the holding force for different pitch values under three operating modes.

11 was 195.3 kN and 167 kN at the pitch of 150 mm and 180 mm, respectively. In general, the holding force decreased sharply with the pitch value when the pitch changed from 150 mm to 180 mm. This could be due to the dislocation of nodes in the model, the reduction of effective contact area, and a sudden drop in the holding force; the increase in the pitch value has little effect on the results. When the pitch was 150 mm and 160 mm, the holding force curves did not change. When the pitch was 160 mm, the holding force was 212.7 kN, and when the pitch was 170 mm, the holding force was 198.7 kN. Overall, the holding force decreased the most in the pitch of 160-170 mm, which was a decrease of about 1.4 kN/mm. When the pitch increased, the results changed slightly, especially in the pitch value range of 190-200 mm. The holding force under operating mode 13 at the pitch of 150 mm and 160 mm was 282.2 kN and 267.4 kN, respectively. When the pitch was in the range of 150-160 mm, the holding force decrease was obvious, showing an average decrease of approximately 1.48 kN/mm. However, when the pitch was in the range of 160-200 mm, the decrease was reduced, especially in the range of 160-170 mm, and changes in the holding force were not obvious; the holding force curves were basically flat. Comparing the three operating modes in Figure 28, it can be seen that the change of the diameter of the wire and the preformed armor rod will have a certain influence on the trend of the holding force, but the three figures generally reflect that when the pitch value is small, the increase of the pitch will significantly reduce the holding force, and when the pitch is large, the holding force is not sensitive to the change of the pitch.

The numerical results of the holding force for different pitch lengths under three operating modes were linearly fitted, and error analysis was carried out, as shown in Figure 29.

As shown in Figure 29, the slopes of linear fitting curves in operating modes 11-13 were -0.7, -0.6, and -0.4, respectively, and the linear fitting in operating mode 11 was the most ideal. According to the error band diagram, the maximum relative error of the holding force in operating modes 11-13 was at the pitch of 180 mm, 200 mm, and 160 mm, having values of 5.51%, 6.40%, and 2.54%, respectively; and the error values were less than 7% in all operating modes. Although the use of simple linear fitting to predict the grip strength has a certain accuracy, but from the overall trend, the use of linear fitting effect is poor, you can try to use other functions to predict the trend of holding force.

When the length of the preformed helical fitting is the same, the smaller the pitch value of the preformed helical fitting, the greater the value of the holding force that can be borne. It has been concluded that when the total length of the preformed helical fitting is certain, and the holding force requirement is satisfied, a smaller pitch value should be selected to ensure sufficient holding force and stable operation of transmission lines.

4) DIAMETER EFFECT ON HOLDING FORCE OF PREFORMED HELICAL FITTING

When the pre-strand pitch size, length, raw materials, and rotation were the same, to meet the experimental abrasive specifications and to eliminate accidental errors, the pre-strand pitches in the range of 150-200 mm were selected for each iteration. A total of 48 operating modes were defined and used to analyze the changing trend of the preformed armor rod holding force. The specific operating modes are presented in Table 8, and the calculation results are shown in Figure 30.

The results indicated that, except for the holding force decrease at certain points, the holding force of the preformed helical fitting increased with the preformed armor rod diameter. In operating mode 14, at the pitch of 170 mm, the holding force increase was obviously linear. The hold-

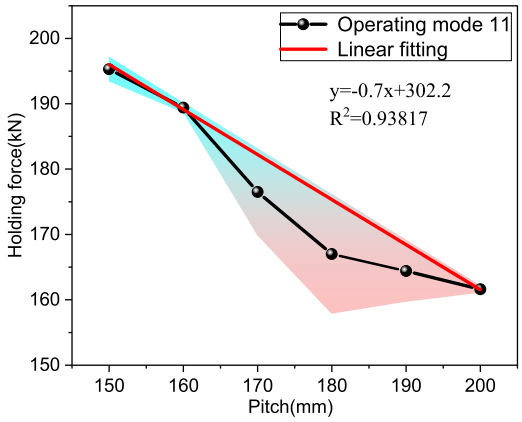

(a) Group 11: linear fitting and error band diagram

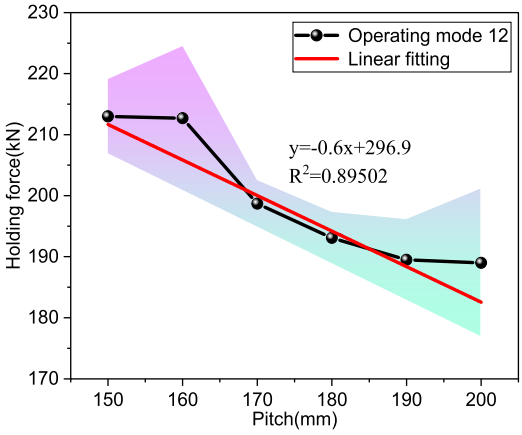

(b) Group 12: linear fitting and error band diagram

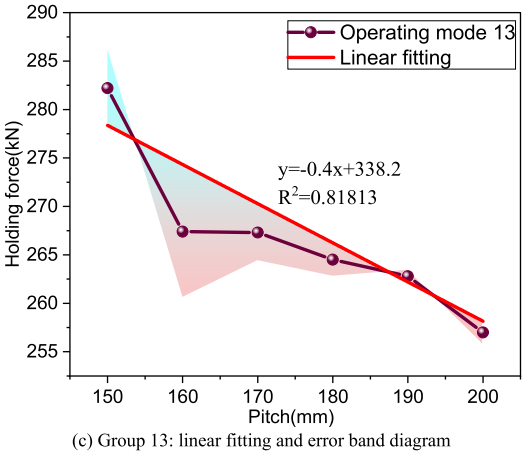

(c) Group 13: linear fitting and error band diagram

FIGURE 29. Linear fitting and error band diagram of the preformed armor rods under various operating modes.

TABLE 8. Finite element model parameters of working conditions 14 and 15.

Group no.	D_w (mm)	D_c (mm)	Mesh size (S_w/S_c(mm))	Pitch length (mm)
14	4.8,5.0 5.2,5.4	15.8	1.0/2.0	150,160 170,180 190,200
15	6.6,6.8 7.0,7.2	20.0		

ing force of the preformed armor rods with a diameter of 4.8 mm and 5.4 mm was 156.4 kN and 191.0 kN, respectively.

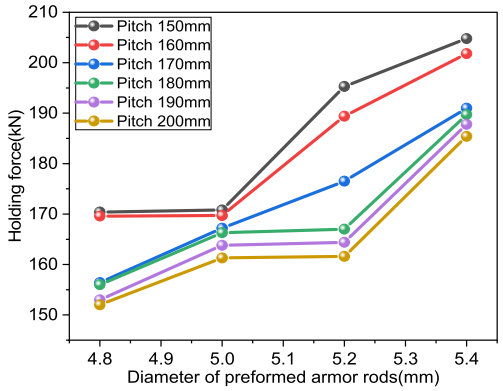

(a) Group 14: holding force versus pitch length diagram

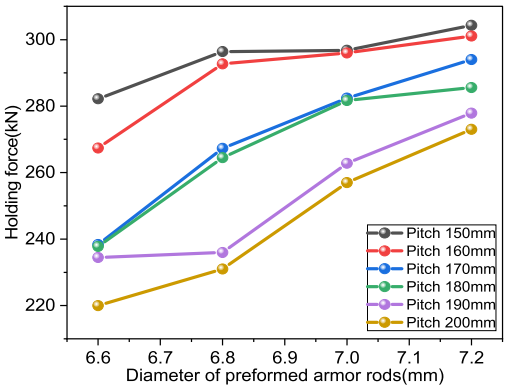

(b) Group 15: holding force versus preformed armor rod diameter diagram

FIGURE 30. Holding forces of the preformed helical fitting fittings for different pitch lengths under different operating modes.

The holding force increased by approximately 5.8 kN when the diameter increased by 0.1 mm; when the diameter was 5.0 mm and 5.2 mm, the change in the holding force was not obvious in the pitch range of 180–200 mm, that is, the holding force curve was almost flat. In addition, the holding force values at the pitch values of 150 mm and 160 mm, 170 mm and 180 mm, and 190 mm and 200 mm were similar, showing a difference of maximally 3%. Specifically, when the diameter was 6.6 mm, the holding force was 238.4 kN and 237.8 kN at the pitch value of 170 mm and 180 mm, respectively, and the difference in the holding force was the smallest. Based on the above results, an appropriate increase in the pre-strand diameter could increase the holding force.

IV. CONCLUSION

In this paper, we studied the holding force of preformed helical fittings and analyzed the effects of different parameters on the holding force from the perspective of structural characteristics using the ABAQUS software. Through the control variable method, the influence of the length, pitch length, forming aperture and armor rod diameter of the preformed helical fitting on the holding force is analyzed.

The main findings of this study can be summarized as follows:

1.The holding force of the preformed helical fitting is inversely proportional to the molding aperture. The holding

force of the preformed helical fitting can be improved by appropriately reducing the molding aperture;

2. When the total length of the preformed helical fitting is constant, the holding force decreases with the increase of the pitch length, so the preformed helical fitting design can be used to reduce the pitch length to improve the holding force;

3.The holding force of the performed helical fitting increases significantly with the armor rod diameter, and the holding force of the performed helical fitting can be improved by increasing the armor rod diameter.

REFERENCES

[1] H. Deng, R. Peng, M. Zhong, R. Yang, Y. Liang, D. Guo, and G. Liu, "A case study of rupture in overhead ground wire twined by armor rod," *Eng. Failure Anal.*, vol. 131, Jan. 2022, Art. no. 105844, doi: 10.1016/J.ENGFAILANAL.2021.105844.

[2] A. Omrani, "Fretting fatigue life assessment of overhead conductors using a clamp/conductor numerical model and biaxial fretting fatigue tests on individual wires," *Fatigue Fract. Eng. Mater. Struct.*, vol. 44, no. 6, pp. 1498–1514, Mar. 2021, doi: 10.1111/FFE.13444.

[3] T. Miranda, R. Badibanga, J. A. Araujo, C. Silva, and J. Ferreira, "Fatigue evaluation of all aluminium alloy conductors fitted with elastomeric and metallic suspension clamps," *IEEE Trans. Power Del.*, vol. 37, no. 1, pp. 539–546, Feb. 2022, doi: 10.1109/TPWRD.2021.3064823.

[4] T. Miranda, "Effect of suspension clamp types on the dynamic bending stress of all aluminium alloy 1120 overhead conductors," *IEEE Trans. Power Del.*, vol. 38, no. 2, pp. 833–841, Apr. 2023, doi: 10.1109/TPWRD.2022.3199680.

[5] J. W. Phillips and G. A. Costello, "Analysis of wire ropes with internal-wire-rope cores," *J. Appl. Mech.*, vol. 52, no. 3, pp. 510–516, Sep. 1985, doi: 10.1115/1.3169092.

[6] W. G. Jiang, J. L. Henshall, and J. M. Walton, "A concise finite element model for three-layered straight wire rope strand," *Int. J. Mech. Sci.*, vol. 42, no. 1, pp. 63–86, Jan. 2000, doi: 10.1016/S0020-7403(98)00111-8.

[7] W. G. Jiang and J. L. Henshall, "A novel finite element model for helical springs," *Finite Elements Anal. Des.*, vol. 35, no. 4, pp. 363–377, Jul. 2000, doi: 10.1016/S0168-874X(99)00076-1.

[8] W. G. Jiang, M. S. Yao, and J. M. Walton, "A concise finite element model for simple straight wire rope strand," *Int. J. Mech. Sci.*, vol. 41, no. 2, pp. 143–161, Jan. 1999, doi: 10.1016/S0020-7403(98)00039-3.

[9] E. Stanova, G. Fedorko, M. Fabian, and S. Kmet, "Computer modelling of wire strands and ropes—Part I: Theory and computer implementation," *Adv. Eng. Softw.*, vol. 42, no. 6, pp. 305–315, Jun. 2011, doi: 10.1016/j.advengsoft.2011.02.008.

[10] E. Stanova, G. Fedorko, M. Fabian, and S. Kmet, "Computer modelling of wire strands and ropes part II: Finite element-based applications," *Adv. Eng. Softw.*, vol. 42, no. 6, pp. 322–331, Jun. 2011, doi: 10.1016/j.advengsoft.2011.02.010.

[11] Y. Han, H. Yong, and Y. Zhou, "The global mechanical response and local contact in multilevel helical structures under axial tension," *Int. J. Mech. Sci.*, vol. 239, Feb. 2023, Art. no. 107886, doi: 10.1016/j.ijmecsci.2022.107886.

[12] D. Zhang and M. Ostoja-Starzewski, "Finite element solutions to the bending stiffness of a single-layered helically wound cable with internal friction," *J. Appl. Mech.*, vol. 83, no. 3, pp. 1–8, Mar. 2016, doi: 10.1115/1.4032023.

[13] L. Xiang, "Elastic-plastic modeling of metallic strands and wire ropes under axial tension and torsion loads," *Int. J. Solids Struct.*, vol. 129, pp. 103–118, Dec. 2017, doi: 10.1016/j.ijsolstr.2017.09.008.

[14] S. Moradi, K. Ranjbar, and H. Makvandi, "Failure analysis of a drilling wire rope," *J. Failure Anal. Prevention*, vol. 12, no. 5, pp. 558–566, Oct. 2012, doi: 10.1007/s11668-012-9596-7.

[15] J. Wu, "The finite element modeling of spiral ropes," *Int. J. Coal Sci. Technol.*, vol. 1, no. 3, pp. 346–355, Sep. 2014, doi: 10.1007/s40789-014-0038-x.

[16] F. Meng, Y. Chen, M. Du, and X. Gong, "Study on effect of inter-wire contact on mechanical performance of wire rope strand based on semi-analytical method," *Int. J. Mech. Sci.*, vols. 115–116, pp. 416–427, Sep. 2016, doi: 10.1016/j.ijmecsci.2016.07.012.

[17] B. Cen, X. Lu, and X. Zhu, "Research of numerical simulation method on vertical stiffness of polycal wire rope isolator," *J. Mech. Sci. Technol.*, vol. 32, no. 6, pp. 2541–2549, Jun. 2018, doi: 10.1007/s12206-018-0511-3.

[18] H. I. Ivanov, N. S. Ermolaeva, J. Breukels, and B. C. de Jong, "Effect of bending on steel wire rope sling breaking load: Modelling and experimental insights," *Eng. Failure Anal.*, vol. 116, Oct. 2020, Art. no. 104742, doi: 10.1016/j.engfailanal.2020.104742.

[19] Y. Chen, F. Meng, and X. Gong, "Full contact analysis of wire rope strand subjected to varying loads based on semi-analytical method," *Int. J. Solids Struct.*, vol. 117, pp. 51–66, Jun. 2017, doi: 10.1016/j.ijsolstr.2017.04.004.

[20] E. A. W. de Menezes and R. J. Marczak, "Comparative analysis of different approaches for computing axial, torsional and bending stiffnesses of cables and wire ropes," *Eng. Struct.*, vol. 241, Aug. 2021, Art. no. 112487, doi: 10.1016/J.ENGSTRUCT.2021.112487.

[21] F. Foti and L. Martinelli, "Mechanical modeling of metallic strands subjected to tension, torsion and bending," *Int. J. Solids Struct.*, vol. 91, pp. 1–17, Aug. 2016, doi: 10.1016/j.ijsolstr.2016.04.034.

[22] J. Said, S. Garcin, S. Fouvry, G. Cailletaud, C. Yang, and F. Hafid, "A multi-scale strategy to predict fretting-fatigue endurance of overhead conductors," *Tribol. Int.*, vol. 143, Mar. 2020, Art. no. 106053, doi: 10.1016/j.triboint.2019.106053.

[23] J. Said, S. Fouvry, G. Cailletaud, C. Yang, and F. Hafid, "Shear driven crack arrest investigation under compressive state: Prediction of fretting fatigue failure of aluminium strands," *Int. J. Fatigue*, vol. 136, Jul. 2020, Art. no. 105589, doi: 10.1016/j.ijfatigue.2020.105589.

[24] G. Liu, W. Zheng, D. Guo, R. Peng, X. Lin, and M. Zhong, "Numerical modeling and analysis of thermal and mechanical behavior for ground wire-clamp system under short-circuit current," *Electr. Power Syst. Res.*, vol. 201, Dec. 2021, Art. no. 107497, doi: 10.1016/J.EPSR.2021.107497.

[25] T. Zhang, W. Zheng, Y. Xie, J. Yuan, T. Xu, P. Wang, G. Liu, D. Guo, G. Zhang, and Y. Liang, "A case study of rupture in 110 kV overhead conductor repaired by full-tension splice," *Eng. Failure Anal.*, vol. 108, Jan. 2020, Art. no. 104349, doi: 10.1016/j.engfailanal.2019.104349.

[26] D. Guo, P. Wang, W. Zheng, Y. Li, J. Li, W. Tang, L. Shi, and G. Liu, "Investigation of sag behaviour for aluminium conductor steel reinforced considering tensile stress distribution," *Roy. Soc. Open Sci.*, vol. 8, no. 8, Aug. 2021, Art. no. 210049, doi: 10.1098/RSOS.210049.

[27] P. H. C. Rocha, "Studies on fatigue of two contacting wires of overhead conductors: Experiments and modeling," M.S. thesis, Dept. Mech. Eng., Univ. Brasilia, Brasília, Brazil, Jan. 2019. [Online]. Available: repositorio.unb.br/handle/10482/35604

[28] I. M. Matos, P. H. C. Rocha, R. B. Kalombo, L. A. C. M. Veloso, J. A. Araújo, and F. C. Castro, "Fretting fatigue of 6201 aluminum alloy wires of overhead conductors," *Int. J. Fatigue*, vol. 141, Dec. 2020, Art. no. 105884, doi: 10.1016/j.ijfatigue.2020.105884.

[29] A. Belkhabbaz, M. Gueguin, F. Hafid, C. Yang, O. Allix, and J.-M. Ghidaglia, "Surrogate model based approach to predict fatigue stress field in multi-stranded cables," *Int. J. Solids Struct.*, vols. 230–231, Nov. 2021, Art. no. 111168, doi: 10.1016/J.IJSOLSTR.2021.111168.

[30] S. Lalonde, R. Guilbault, and S. Langlois, "Numerical analysis of ACSR conductor–clamp systems undergoing wind-induced cyclic loads," *IEEE Trans. Power Del.*, vol. 33, no. 4, pp. 1518–1526, Aug. 2018, doi: 10.1109/TPWRD.2017.2704934.

[31] M. Frigerio, P. B. Buehlmann, J. Buchheim, S. R. Holdsworth, S. Dinser, C. M. Franck, K. Papailiou, and E. Mazza, "Analysis of the tensile response of a stranded conductor using a 3D finite element model," *Int. J. Mech. Sci.*, vol. 106, pp. 176–183, Feb. 2016, doi: 10.1016/j.ijmecsci.2015.12.015.

[32] L. Xin, "Application of pre–twisted electric fittings in transmission lines," *Sci. Technol. Consulting Herald*, vol. 16, p. 31, Jun. 2007, doi: 10.16660/j.cnki.1674-098x.2007.16.025.

[33] L. Xingning and Y. Shengping, "Design and characteristic analysis of pre–twisted power fittings," *Sci. Technol. Inf.*, vol. 1, pp. 516–523, Jan. 2011.

[34] X. Xuetai, "Novel power fittings-preformed armor rod," *Electr. World*, vol. 40, no. 11, pp. 22–23, Nov. 1999.

[35] W. Jiancheng, D. Yuming, Y. Wengang, S. Jiajun, L. Long, and Z. Qiuhua, "Parameterized finite element modeling of expanded conductor," *Electr. Power Sci. Eng.*, vol. 31, no. 7, pp. 18–74, Jul. 2015, doi: 10.3969/j.issn.1672-0792.2015.07.014.

[36] C. Jolicoeur and A. Cardou, "A numerical comparison of current mathematical models of twisted wire cables under axisymmetric loads," *J. Energy Resour. Technol.*, vol. 113, no. 4, pp. 241–249, Dec. 1991, doi: 10.1115/1.2905907.
[37] W. Shilong, R. Weijun, Z. Jie, M. Jianjun, and L. Chuan, "Study on 3D curve model of multi-stranded wire helical springs," *China Mech. Eng.*, vol. 18, no. 11, pp. 1269–1272, Jun. 2007.
[38] W. Shilong, X. Hong, Z. Jie, and L. Song, "Research on differential geometry of stranded wire helical springs," *China Mech. Eng.*, vol. 20, no. 17, pp. 2089–2093, Sep. 2009.

LV ZHONGBIN was born in China. He is with the State Grid Henan Electric Power Research Institute. His research interests include security and disaster prevention and the control of transmission lines.

TAO YAGUANG was born in China. He is with the State Grid Henan Electric Power Research Institute. His research interests include security and disaster prevention and the control of transmission lines.

LIU XIAOHUI was born in China. He joined the School of Civil Engineering, Chongqing Jiaotong University, in 2011, where he is currently a Professor. His research interests include the galloping of transmission line and dynamics of structures.

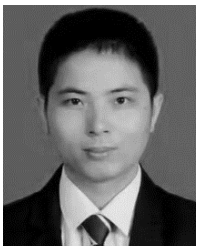

YE ZHONGFEI was born in China. He is with the State Grid Henan Electric Power Research Institute. His research interests include security and disaster prevention and the control of transmission lines.

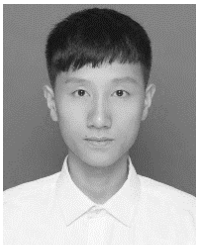

LI HONGPAN was born in China. He is currently pursuing the degree with Chongqing Jiaotong University, under the supervision of Xiaohui Liu. His research interest includes the mechanical properties of pre-strand fittings.

SUN YUNTAO was born in China. He is with Nanjing Electric Power Fittings Design and Research Institute Company Ltd., where he is currently a Senior Engineer. His research interests include transmission line designs and structural analysis.

YAN BO was born in China. He joined the Department of Engineering Mechanics, Chongqing University, in 1988, where he is currently a Professor. His research interests include solid mechanics and engineering mechanics.